https://doi.org/10.5194/egusphere-2023-2102
Preprint. Discussion started: 5 October 2023

Active microbial sulfur cycling in 13,500-year-old lake sediments

Jasmine S. Berg[1a*], Paula C. Rodriguez[2], Cara Magnabosco[2], Longhui Deng[1b], Stefano M. Bernasconi[2], Hendrik Vogel[3], Marina Morlock[3c], Mark A. Lever[1d]

[1]Department of Environmental Systems Science, ETH-Zurich, 8049 Zurich, Switzerland

[2]Department of Earth Sciences, ETH-Zurich, 8049 Zurich, Switzerland

[3]Institute of Geological Sciences & Oeschger Centre for Climate Change Research, University of Bern, 3012 Bern, Switzerland

*corresponding author: jasmine.berg@unil.ch

[a] Present address: Department of Geosciences and Environment, University of Lausanne, 1015 Lausanne, Switzerland

[b] Present address: School of Oceanography, Shanghai Jiao Tong University, Shanghai 200240, China

[c] Present address: Department of Ecology and Environmental Sciences, Umeå Universitet, 901 87 Umeå, Sweden

[d] Present address: Marine Science Institute, University of Texas at Austin, Port Aransas, TX 78373, USA

keywords: *sulfur cycling, sulfur isotopes, organic sulfur, early diagenesis, lake sediment, meromictic, Holocene, euxinic*

https://doi.org/10.5194/egusphere-2023-2102
Preprint. Discussion started: 5 October 2023

ABSTRACT

The addition of sulfur (S) to organic matter to form organosulfur compounds is generally thought to protect organic matter from microbial degradation and promote its preservation. While most microbial sulfur cycling occurs in sulfate-rich sediments above the sulfate-methane transition zone, recently discovered active sulfur cycling in deeper sulfate-poor environments may have a yet-unquantified impact on the mineralization of organic matter. Here we investigated the fate of buried S-compounds down to 10-m sediment depth representing the entire ~13.5 kya history of the sulfate-rich alpine Lake Cadagno. Chemical profiles of sulfate and sulfur reveal that these oxidized species are depleted at the sediment surface with the concomitant formation of iron sulfide minerals. An underlying aquifer provides a second source of sulfate and other oxidants to the deepest and oldest sediment layers generating an inverse redox gradient. At both sulfate depletion zones, isotopes of chromium-reducible sulfur (CRS) and humic-bound sulfur are highly negative (-30 to -65 per mil) compared to background sulfate suggesting ongoing microbial sulfur cycling. Interestingly, humic-bound S from intermittent sediment layers within the sulfate-depleted methanogenesis zone consistently exhibits a lower $\delta^{34}S$ than CRS in lacustrine deposits but a higher $\delta^{34}S$ than CRS in terrestrial deposits, which could possibly be due to different reactivities of organic matter types (lacustrine versus terrestrial origin) to sulfide or the ability of microorganisms to form/degrade organic S. Although sulfate concentrations are extremely low between the sulfate depletion zones, *dsrB* gene libraries reveal a huge potential for microbial sulfur reduction throughout the sediment column.

https://doi.org/10.5194/egusphere-2023-2102
Preprint. Discussion started: 5 October 2023

1. INTRODUCTION

The biological sulfur cycle exerts an important control on organic matter burial and thus plays a major role in the global cycling of carbon in addition to the elements O, N and Fe. In anoxic marine sediments, microbial reduction of sulfate (SO_4^{2-}) to hydrogen sulfide (ΣH_2S) is quantitatively the most important respiration reaction, remineralizing 12-29% of the total organic carbon flux to the seafloor (Jørgensen, 1982; Bowles et al., 2014). Even in freshwater systems, where sulfate concentrations are typically 100-1,000 times lower than in seawater, high rates of microbial sulfate reduction can be sustained by rapid reoxidation of ΣH_2S by Fe^{III}, Mn^{IV}, and possibly by redox-active organic substances, e.g. certain humic acids (Pester et al., 2012).

Sulfur isotopic fractionation can provide important insights into microbial sulfur cycling, especially where consumption of sulfate cannot be inferred from concentration gradients. Microorganisms preferentially reduce light (^{32}S) over heavier (^{34}S) sulfate generating isotopic fractionations (3 to 75 ‰) between sulfate and hydrogen sulfide which vary in magnitude with specific metabolic activity and sulfate concentration (e.g. (Habicht and Canfield, 1997; Detmers et al., 2001; Brunner and Bernasconi, 2005; Sim et al., 2011; Bradley et al., 2016)). Biogenic sulfide reacts readily with free Fe^{2+} to form iron sulfide (FeS) and eventually pyrite (FeS_2), whose widespread occurrence in the geological record helps facilitate reconstruction of past environmental conditions (Canfield, 2004; Johnston, 2011; Paiste et al., 2020). While pyrite $\delta^{34}S$ values supposedly record the S isotopic composition of porewater fluids, major isotopic shifts (between 10 and 40‰) have been observed between sedimentary pyrite and dissolved H_2S (Chanton et al., 1987; Canfield et al., 1992; Brüchert and Pratt, 1996; Raven et al., 2016; Lin et al., 2016). These discrepancies have been explained by processes such as sediment remobilization, bioturbation, and even post-depositional sediment-fluid

https://doi.org/10.5194/egusphere-2023-2102
Preprint. Discussion started: 5 October 2023

interactions which can impact $\delta^{34}S$ records during diagenesis (Fike et al., 2015). A large discrepancy has also been observed (5‰–30‰) between experimental microbial fractionation and the isotopic composition of environmental pyrites (Habicht and Canfield, 2001). One confounding process in the S isotopic cycle is microbial disproportionation, which produces heavy sulfate and light sulfide (Canfield and Thamdrup, 1994). Still, extreme isotope depletion of sulfides (> 70‰) generated by sulfate reduction alone has been theoretically modeled (Brunner and Bernasconi, 2005) and identified in pure cultures (Johnston et al., 2007; Canfield et al., 2010; Sim et al., 2011) and in deep sediments (Wortmann et al., 2001) and crustal rocks (Lever et al., 2013) suggesting that we do not yet fully understand the effects of sulfate-reducing microbial communities nor sulfide mineral crystallization pathways on isotope fractionation (Fike et al., 2015).

While S isotopes in pyrite are most often used as a marker for sulfate reduction, organic S constitutes the biggest S pool in many freshwater sediments (Mitchell et al., 1981; Nriagu and Soon, 1985; Urban et al., 1999). This organic S originates from both the settling of seston material and the microbial reduction of water column-derived sulfate to hydrogen sulfide, which then reacts with sedimentary organic matter (David and Mitchell, 1985; Rudd et al., 1986). The sulfurization of organic matter tends to promote its resistance to microbial degradation thus contributing significantly to long-term preservation of organic carbon in sediments (Damsté and De Leeuw, 1990; Hebting et al., 2006), and to petroleum formation (Orr and Damsté, 1990). Though it is likely that some microorganisms are capable of degrading fractions of this organic S pool, their activity and identity is unknown.

Recently, the metabolic capacity for sulfur cycling has been expanded across phylogenetic groups with the identification of specific marker genes across taxa previously unknown for this metabolism (Anantharaman et al., 2018). Although the presence of such genes must be interpreted with caution, their distribution across environments can help illuminate

https://doi.org/10.5194/egusphere-2023-2102
Preprint. Discussion started: 5 October 2023

putative sulfur reducing and sulfur oxidizing communities within diverse ecosystems. *soxB*, which encodes the thiosulfohydrolase of the Sox enzyme system, is one such marker gene, and has been widely employed to characterize sulfur-oxidizing bacteria (SOB) diversity (Meyer et al., 2007). Another example is *dsr*AB, which encodes dissimilatory sulfite reductase, an enzyme that catalyzes the reduction of sulfite to sulfide and is used by all known sulfate reducers (Klein et al., 2001).

Because microbial sulfur cycling appears to be of continued ecological and geochemical significance in sulfate-depleted marine sediments (Holmkvist et al., 2011; Brunner et al., 2016; Pellerin et al., 2018a), such processes may likewise occur in the sulfate-depleted sediments of lakes. Here we investigate the potential for microbial sulfur cycling in Lake Cadagno, which is an intermediate system between freshwater and seawater, due to its elevated sulfate concentrations (1-2 mM). We combine chemical quantifications and isotopic analyses on major S and C phases with molecular sequencing on the complete sedimentary sequence of Lake Cadagno. We hypothesize that the extent of microbial sulfur cycling is related to organic matter quality (lacustrine vs. terrestrial origin) as well as past redox changes that are preserved in the sedimentary record, and that local differences in biogeochemistry control the formation of organic S versus iron sulfide minerals and composition of S isotopes within these pools.

2. METHODS

2.1 Geological setting

The meromictic Lake Cadagno, located in the Swiss Alps, contains 1-2 mM dissolved sulfate originating from the dissolution of dolomite bedrock via subaquatic springs. Since its formation ~13.5 kya, Lake Cadagno has undergone a complex redox history, transitioning from seasonal stratification around 12.5 kya to complete euxinia about 10.9 kya (Wirth et al., 2013; Berg et al., 2022). Preliminary analyses of sulfur phases in surface (Urban et al., 1999) and deep

https://doi.org/10.5194/egusphere-2023-2102
Preprint. Discussion started: 5 October 2023

sediments (Berg et al., 2022) suggest an active dissimilatory sulfur cycle below the sulfate depletion zone (SDZ).

All Lake Cadagno deep sediment core sampling, geochemical analyses of sediment and porewater, and DNA extractions were performed as described in (Berg et al., 2022). Additional samples for sulfate isotope analyses were obtained in June 2020 from one surface spring (at SwissGrid coordinates 2'697'763, 1'155'959) and one subaquatic spring at approximately 5 m depth (2'697'521, 1'156'044) located on the south side of the lake.

2.2 Solid-phase sulfur extractions

Sequential sulfur extractions were performed based on the protocol of Ferdelman et al. (1991). First, elemental sulfur was extracted under N_2 atmosphere three times with degassed 100% methanol. During each step the methanol-sample mixture was sonicated for 10 min in an ice bath, centrifuged, and then the methanol was pipetted into a clean vial. Methanol extracts were analyzed by ultrahigh pressure liquid chromatography (UPLC) using a Waters Acquity H-class instrument with an Aquity UPLC BEH C18, 1.7 µm, 2.1 × 50 mm column (Waters, Japan) and a PDA detector (absorbance wavelength set to 265 nm). The injection volume was 10 µl with methanol as eluent flowing at 0.2 ml min^{-1}. Elemental sulfur eluted at 4.14 min.

Next, humic acids were extracted 3 times, or until the supernatant was clear, with degassed 0.1 M NaOH and collected in 50 ml Falcon tubes. Silicates were precipitated from the base extracts by addition of saturated NaCl solution (5 mL per 45 mL extract) and removed by centrifugation and decanting. The basic extract then was acidified to pH 1.5 with concentrated HCl, allowed to stand at 4°C overnight, and then centrifuged. The humic acid fraction was washed three times with distilled water to remove excess salts prior to drying and reserved for C, N, and S analysis.

https://doi.org/10.5194/egusphere-2023-2102
Preprint. Discussion started: 5 October 2023

Finally, acid-volatile sulfur (AVS) and chromium-reducible sulfur (CRS) were extracted from the remaining sediment using the two-step acid Cr-II method (Fossing and Jørgensen, 1989; Kallmeyer et al., 2004). For the AVS fraction, 6 N HCl was added to sediment in a reaction flask under N_2 atmosphere and H_2S was trapped by bubbling through a 5% Zn-acetate solution for 2 h. The CRS fraction was subsequently obtained by replacing the Zn-acetate trap, adding 20 ml of DMSO and 16 ml of $CrCl_2$ solution, and reacting again for 2 h. AVS and CRS fractions collected as ZnS were quantified photometrically as above and then pelleted by centrifugation, rinsed with MilliQ, and dried at 50°C prior to $\delta^{34}S$ analyses as described below.

Concentrations and isotope compositions of sulfur in the AVS, CRS and HAS fractions as well as in sulfate from porewater, a subaquatic spring, and two surface springs, were determined using a Flash-EA 1112 (ThermoFisher) coupled to an isotope ratio mass spectrometer (IRMS, Delta V, ThermoFisher) by addition of vanadium pentoxide as a catalyst. Isotope ratios are reported in the conventional δ -notation with respect to the Vienna-Cañon Diabolo Troilite (VCDT) standard for sulfur. The system was calibrated for sulfur using the international standards for sulfide and sulfate: IAEA-S1 ($\delta^{34}S$ = -0.3), IAEA-S2 ($\delta^{34}S$ = +22.67), IAEA-S3 ($\delta^{34}S$ = -32.55) and IAEA-SO5 ($\delta^{34}S$ = +0.49), IAEA-SO6 ($\delta^{34}S$ = -34.05), NBS-127 ($\delta^{34}S$ = +21.1), respectively. Reproducibility of the measurements was better than 0.2‰.

2.3 DNA extraction and sulfur-cycling gene analyses

DNA was extracted according to lysis protocol II of (Lever et al., 2015) as outlined in (Berg et al., 2022). The B subunit of the *dsr*AB gene was PCR-amplified using the low-degeneracy *dsr*B F1a-h / 4RSI1a-f primer mixtures from (Lever et al., 2013). *sox*B genes were amplified using the recently designed *sox*B-837F1a-l / *sox*B_1170R1a-g low-degeneracy primer mixtures

https://doi.org/10.5194/egusphere-2023-2102
Preprint. Discussion started: 5 October 2023

(Deng et al., 2022). Quantitative PCRs (qPCR) with these low-degeneracy primers consisted of the same reaction mixtures as for *dsr*B and were performed on a LightCycler 480 II system using the instrument settings and reagent mixtures outlined in (Jochum et al., 2017). The thermal cycler conditions were (1) enzyme activation and initial denaturation at 95°C for 5 min; (2) 60 cycles of (a) denaturation at 95°C for 30 s, (b) annealing at 60°C for 30 s, (c) elongation at 72°C for 25 s, and (d) fluorescence acquisition at 80°C for 5 s; and (3) a stepwise melting curve from 60 to 95°C to check for primer specificity. Plasmids that carry the *dsr*B and *sox*B genes from *Desulfotomaculum carboxydivorans* and *Thiobacillus denitrificans*, respectively, were applied as qPCR standards.

*dsr*B gene sequences were phylogenetically annotated using the ARB software (www.arb-home.net) based on an updated version of the *dsr*AB database published in (Müller et al., 2015). This database was expanded by adding *dsr*AB gene sequences from since then published metagenomes, as well as a closest BLAST hit to *dsr*B gene sequences detected in Lake Cadagno. The phylogenetic annotation was based on a *dsr*AB gene bootstrap tree that was built by ARB Neighbor-Joining with Jukes-Cantor correction using diverse *dsr*AB reads that covered the entire *dsr*B gene amplicon sequence and were at least 750 bp in length. The shorter amplicon sequences from Lake Cadagno, as well as closest BLAST hits that were <750 bp long were added using the ARB Parsimony option combined with a newly designed, amplicon-specific *dsr*B filter that removed hypervariable regions.

3. RESULTS

3.1 Sulfur Geochemistry in Lake Cadagno sediments

The complete sedimentary sequence from Lake Cadagno is approximately 950 cm long, covering a period of ~13.5 kya (Berg et al., 2022). Sediments are characterized by relatively fine grained pelagic lacustrine sediments interspersed with frequent coarser-grained flood- and

https://doi.org/10.5194/egusphere-2023-2102
Preprint. Discussion started: 5 October 2023

mass movement-derived deposits containing remobilized littoral lake and terrestrial sediment in the upper 790 cm, underlain by light-colored fine-grained deposits of late glacial origin (Fig. 1). The sediment can thus be divided into three distinct lithostratigraphic units representing an early oxic lake (950-790 cm; 13.5 to 12.5 kya), a redox transition interval (790-760 cm; 12.5 to 10.9 kya), and the euxinic period (above 760 cm; 10.9 kya to present). High-resolution mapping of element geochemistry on split core surfaces (Fig. 1) reveals that the accumulation of sulfur is restricted to sediments deposited after the onset of periodic to permanent reducing conditions. Fe and S were normalized against Ti, which represents the lithogenic fraction unaltered by redox processes in the aquatic environment. The correlation between S/Ti and Fe/Ti suggests the presence of authigenic iron sulfide phases. The largest S excursions are located at 173 and 600 cm depth, but these do not appear related to sediment origin (lacustrine vs. terrestrial).

Figure 1| Lithological profile determined from a composite core image of the sedimentary sequence retrieved from Lake Cadagno. XRF profiles of S/Ti and Fe/Ti. Changes in lake redox chemistry are denoted by dashed lines.

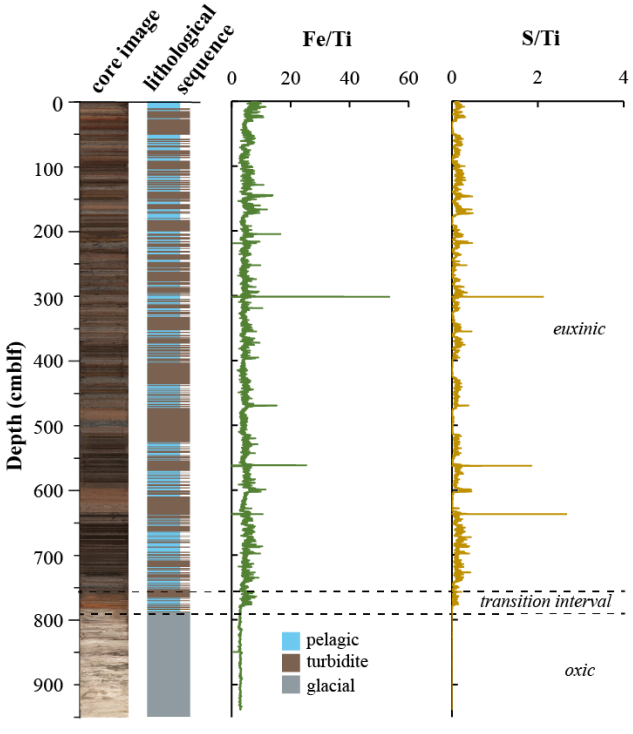

To obtain further insights into sulfur redox cycling in these sediments, major solid sulfur phases were quantified (Fig. 2A). Elemental sulfur (S^0) is the most abundant solid sulfur phase in surface sediments at 300 µmol/g dry sediment. The parallel decrease in S^0 and Fe^{III} with depth indicate

https://doi.org/10.5194/egusphere-2023-2102
Preprint. Discussion started: 5 October 2023

increasingly reducing conditions. Sulfide and Fe^{2+} released from reduction reactions precipitate as AVS (mostly amorphous FeS and mackinawite) which exhibits a peak at 10 cm depth, in parallel with a peak in humic acid-bound S (HAS), defined as the fraction of sulfur extractable in 0.1 M NaOH. Below this depth, AVS, S^0, and HAS decrease at the expense of CRS formation. In the deeper sediments, S^0 and AVS are not detectable whereas HAS concentrations are relatively constant (0.15-1.5 µmol/g dry sed) and CRS levels fluctuate widely (10-270 µmol/g dry sed). The highest concentrations of CRS and HAS are consistently associated with lacustrine deposits and HAS is the dominant pool of sulfur in most of the deep euxinic sediments despite the presence of excess free Fe^{2+} and Mn^{2+} favoring formation of metal sulfides (Fig. 2B). There is an exceptionally high CRS content in only a handful of these deposits, especially those overlying thick turbidites.

https://doi.org/10.5194/egusphere-2023-2102
Preprint. Discussion started: 5 October 2023

224 At 760 cm, a second SDZ has been described based on an upwards-diffusing gradient
225 of sulfate thought to originate from a subterranean aquifer (Berg et al., 2022). The change in
226 redox conditions at 775 cm depth is marked by a small peak in AVS (9 µmol/g dry sed) and S^0
227 (23 µmol/g dry sed). Due to prevailing oxidizing conditions, late glacial sediments below 790
228 cm are poor in reduced sulfur and organic matter but contain some iron oxides and up to 200
229 µmol/l sulfate in porewaters (Fig. 2B). These sulfate concentrations are much lower than

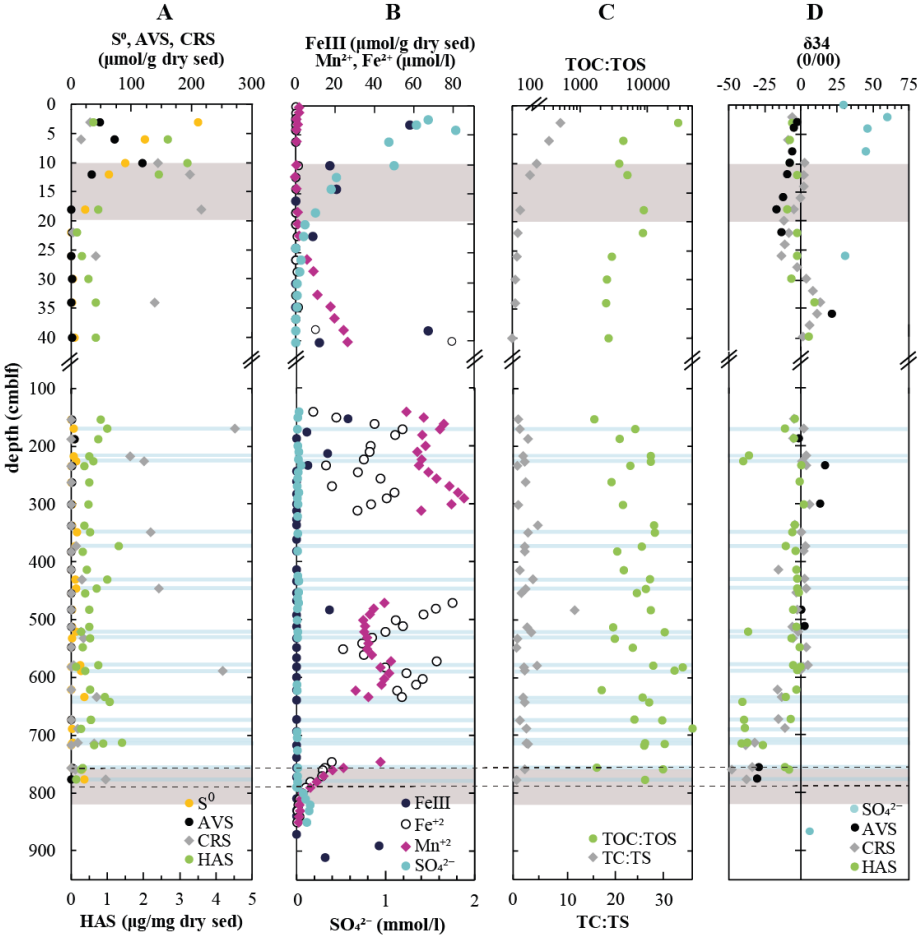

Figure 2| Geochemistry of major solid-phase sulfur pools (A) along with metals and dissolved species (B) involved in sulfur cycling in the sediment column of Lake Cadagno. (C) Ratios of total inorganic and organic carbon and sulfur along with (D) isotope ratios of major sulfur pools. Based on previous geochemical analyses (Berg et al 2022), the sulfate depletion zones have been shaded in gray and lacustrine deposits have been shaded in blue. HAS is represented in µg because of its unknown molecular weight. Note the break in the y-axis.

https://doi.org/10.5194/egusphere-2023-2102
Preprint. Discussion started: 5 October 2023

concentrations of sulfate in lake bottom water (990 µmol/l), but in the same general range as a subaquatic spring (268 µmol/l) and a surface spring (166 µmol/l).

Ratios of C to S are expected to change when sulfide reacts with organic matter forming organic S, and when microorganisms preferentially degrade organic carbon and leave behind organic S. TC:TS decreases from 9 at the surface to about 1.5 at 20 cm depth and remains relatively constant throughout the deeper sediments (Fig. 2C). Most of this carbon is in organic form, with measurable contributions of total inorganic carbon (TIC) present only in surface sediment and again at 400 cm depth (<2 wt%; Fig. S1). In contrast, most sulfur is present in inorganic form and thus TOC:TOS exhibits a very different behavior (Fig. 2C). These values should be interpreted with caution as measured TOS represents a very small fraction of TS (Fig. S1) and minor fluctuations can therefore produce extremely large variations in TOC:TOS ratios. TOC:TOS varied widely and no trends were observeable with depth though ratios were, on average, significantly ($p < 0.001$, Student's t-test) higher in lacustrine deposits (13,372 ± 8686) than in mass movement deposits (5814 ± 5432).

$^{34}S/^{32}S$ isotope ratios of major sulfur phases can indicate the degree that microbial activity impacts various sedimentary S pools. Sufficient sulfate for isotopic analyses was only obtained from five surface samples and by pooling porewater from the entire late glacial sediment sequence (790-910 cm). Sulfate in the upper sediments is highly enriched in ^{34}S, increasing from 24 ‰ in the bottom waters to 60 ‰ within the upper 2 cm suggesting that this is the zone of maximal sulfate reduction. This zone coincides with the highest rates of anaerobic oxidation of methane (AOM) as inferred from methane concentrations and ^{13}C-DIC signatures (Schubert et al., 2011). Previously measured $\delta^{34}S$-sulfate profiles exhibit increasing enrichment in ^{34}S down to the SDZ (Fig. S2). Our sulfate $\delta^{34}S$ measurements were in a similar range, but the depth profile could not be resolved due limitations in extractable porewater volumes and low sulfate concentrations. In the deep glacial sediments, the sulfate isotopic signature is very

https://doi.org/10.5194/egusphere-2023-2102
Preprint. Discussion started: 5 October 2023

light (+7‰), which is more similar to values measured in subaquatic (+12‰) and surface (+15‰) springs.

Consistent with microbial production of sulfide from sulfate reduction, sulfide in Lake Cadagno sediments is generally depleted in ^{34}S relative to sulfate in the overlying water column (Fig. S2). Here we did not obtain sufficient dissolved sulfide ($\sum H_2S$) for isotope analyses, but previously measured profiles reveal light (-17‰) sulfide in the water column which becomes increasingly heavy (up to +9‰) in the upper SDZ before concentrations decrease to detection limits due to reaction with metals (Fig. S2). In contrast, $\delta^{34}S$-AVS becomes progressively lighter in surface sediments exhibiting a minimum of -16‰ within the upper SDZ. In the mid-column sediments, $\delta^{34}S$-AVS fluctuates between -9‰ and +17‰ with no discernible trend, but becomes highly negative in the deep SDZ, exhibiting values as low as -34‰. CRS is more depleted in ^{34}S than AVS at most depths, except for in the upper SDZ where $\delta^{34}S$-CRS values are enriched by ~2‰ relative to $\delta^{34}S$-AVS. In the deep SDZ, extremely light CRS values are observed down to -47.5‰, which is equivalent to a fractionation of 54‰ compared to deep porewater sulfate. $\delta^{34}S$-HAS values fluctuate much more widely than AVS and CRS, varying between 0‰ and -41‰ down to 750 cm depth and exhibiting negative excursions in euxinic mid-column sediments around 225, 520, and 640-720 cm. These ^{34}S-HAS values are significantly lighter ($p < 0.01$, Wilcoxon Signed-Rank test) than CRS values in respective sediment layers, and the most negative $\delta^{34}S$-HAS values are associated with lacustrine deposits. In fact, ^{34}S-HAS in lacustrine layers is significantly lighter ($p < 0.01$, Student's t-test) than that from mass-movement deposits.

https://doi.org/10.5194/egusphere-2023-2102
Preprint. Discussion started: 5 October 2023

3.2 Genetic potential for microbial sulfur cycling

Abundances of sulfur-cycling microorganisms in the Lake Cadagno sediment column were assessed by qPCR of functional genes for sulfate reduction (*dsr*B) and sulfur oxidation (*sox*B) (Fig. 3). Copy numbers of *dsr*B decrease by one order of magnitude, from 4.23 x 10^8 copies/g wet sediment at the surface to 7.17 x 10^6 copies/g wet sediment at 44 cm depth. Gene copy numbers in the sulfate-depleted sediments from 35 to 760 cm depth remain relatively constant between 1.58 x 10^6 and 2.9 x 10^7 copies/g wet sediment. Within the deep SDZ at around 810 cm depth, *dsr*B copy numbers reach a minimum of 3.10 x 10^3 copies/g sediment before increasing again to 2.77 x 10^4 copies/g sediment in parallel with increasing sulfate concentrations (Fig. 2B).

Figure 3| Depth profiles of *dsr*B and *sox*B gene copy numbers. Copies of both genes were detectable by qPCR in all samples targeted. Shaded gray regions indicate sulfate-methane transition zones.

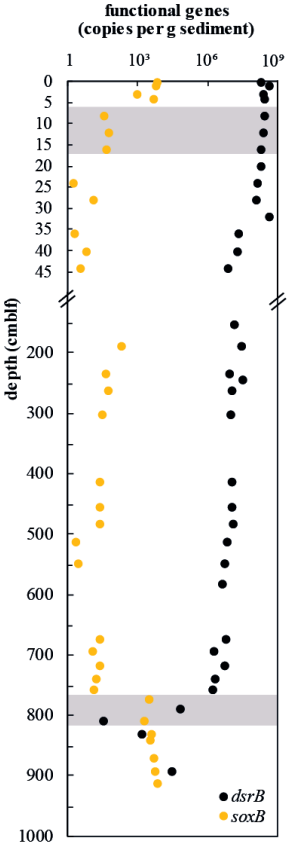

Surprisingly, *sox*B was detectable (up to 6.45 x 10^3 copies/g sediment) in the reducing surface sediments of Lake Cadagno, down to the upper SDZ. In mid-column sediments, sulfur oxidation gene copies remained on the order of 10^1-10^2 before increasing again below 760 cm to 6.59 x 10^3 copies/g sediment. This increase in sulfur oxidation potential matches the oxidizing conditions in deep glacial sediments revealed by the presence of Fe-oxides, elemental sulfur, and sulfate (Fig. 2A&B). It also makes up a large part of the total metabolic potential as 16S qPCR data indicate that microbial population size plummets at 700 cmblf (Berg et al., 2022).

3.3 Diversity of sulfate-reducing microorganisms

https://doi.org/10.5194/egusphere-2023-2102
Preprint. Discussion started: 5 October 2023

Sequencing of the sulfate reduction gene (*dsr*B) revealed a wide diversity of potential sulfate reducers in Lake Cadagno sediments (Fig. 4). The majority of sequences could not be classified beyond the supergroup level, indicating that these are novel lineages. Overall, the sulfate reducers identified in our gene amplicon libraries were consistent with those identified in 16S rRNA gene libraries (Berg et al., 2022). The community profile shows a clear differentiation between surface sediment and deeper sulfate-depleted layers, and there is a clear decrease in species richness with depth and sediment age.

Similar to other sulfate-rich sedimentary environments, Lake Cadagno surface sediments harbor highly abundant (>80% relative abundance) Deltaproteobacteria belonging to

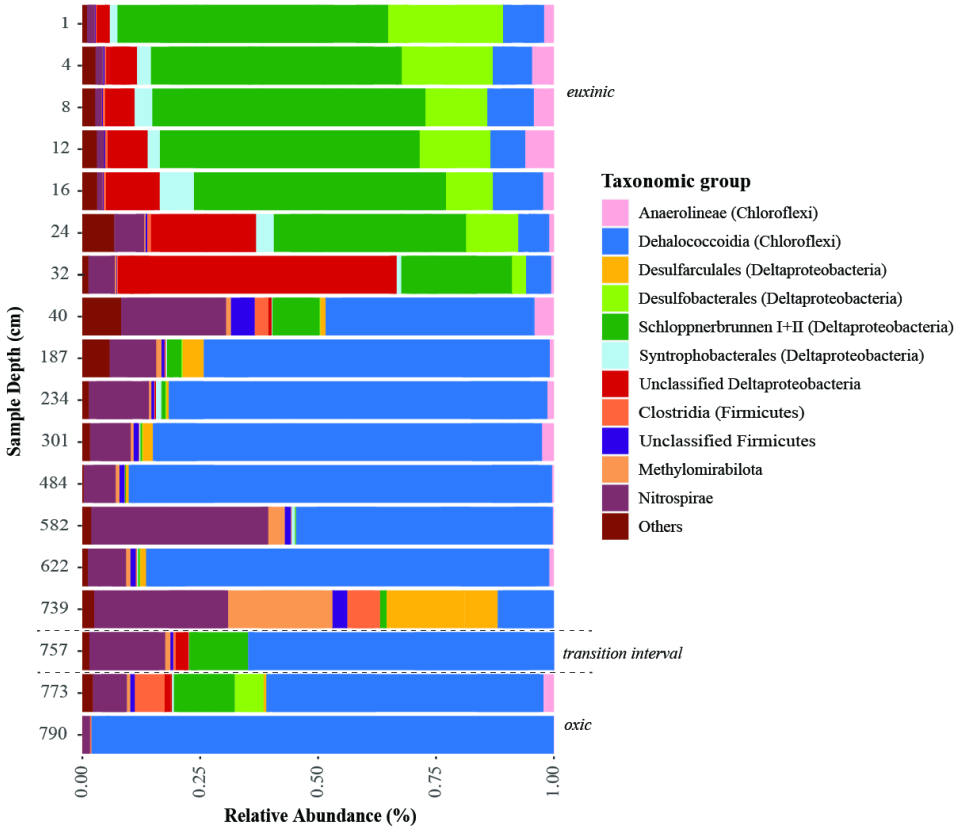

Figure 4| Taxonomic classification of functional genes *dsrB* recovered from the Lake Cadagno sediment depth. Sediment geological transitions are indicated with dashed lines.

https://doi.org/10.5194/egusphere-2023-2102
Preprint. Discussion started: 5 October 2023

uncultured members of the order Desulfobacterales, clade Schlöppnerbrunnen I + II (originally identified in peatland soils), and other unclassified Deltaproteobacteria. In addition, reads belonging to the genera *Desulfobulbus*, *Desulfovibrio*, *Desulfomonile*, of which members are known to also disproportionate sulfur intermediates (Cypionka et al., 1998; Slobodkin and Slobodkina, 2019), are abundant (44000 reads).

Below the SDZ at 40 cm there is a shift in the sulfate-reducing microbial assemblage toward the dominance of uncultivated Chloroflexi. Members of this phylum have so far not been demonstrated to perform dissimilatory sulfur cycling but Chloroflexi *dsrB* sequences have been found in sediments (e.g. Vuillemin et al., 2020; Liu et al., 2022). A second compositional shift occurs in deeper layers around the redox transition interval at 739 cm depth. Genes for sulfate reduction there affiliate with the orders Clostridiales, Dehalococcoidia, Methylomirabilales, and the phylum Nitrospirae. Sulfate reducers belonging to the class Deltaproteobacteria also reappear close to the redox transition but are distinct from those in surface sediments, affiliating mostly with the species *Desulfoarculus baarsii* (classified within the order Desulfarculales). In the deep glacial sediment (> 790 cm), the diversity of microbial sulfate-reducers is reduced (98% of *dsr*B sequence reads) to Chloroflexi from the classes Anaerolineae and Dehalococcoidia.

4. DISCUSSION

4.1 Evidence for continued sulfur cycling in sulfate-depleted sediments

The relatively heavy isotopic signature of sulfate in Lake Cadagno bottom waters (+24 ‰) compared to source waters in subaquatic (+12‰) and surface springs (+15‰) indicate active sulfate reduction in the anoxic lower part of the water column. The $\delta^{34}S$ values of sulfate in the Lake Cadagno springs are the same as those of other springs in the Valle Leventina (Steingruber

https://doi.org/10.5194/egusphere-2023-2102
Preprint. Discussion started: 5 October 2023

et al., 2020) indicating dissolution of gypsum/dolomite in the marine evaporites from the Middle Triassic as the main source (Bernasconi et al., 2017).

Microbial sulfur cycling in the upper sediment appears to be primarily driven by uncultured groups of bacteria with unexplored genetic potential. While sulfate reduction is linked primarily to organic matter degradation rather than anaerobic methane oxidation (Berg et al., 2022), some of these sulfate reducers, such as the facultative secondary fermenters *Syntrophobacter*, may be supplying substrates for methanogenesis. We also identified several bacterial genera potentially involved in sulfur disproportionation and detected genes for sulfur oxidation, despite the anoxic nature of these sediments.

While sulfate is depleted below 30 cm depth, sulfate or other intermediate sulfur species may still be regenerated by reactions with metal oxides and fuel microbial sulfur cycling. In the euxinic mid-column sediments, the low sulfate concentrations of 0-25 µmol/l are potentially due to contamination of subsurface porewaters with sulfate-rich bottom waters during sediment coring. Nevertheless, the abundance of *dsr*B genes belonging to a wide diversity of sulfate-reducing microorganisms reveals that sulfate/sulfur reduction likely continues throughout the sulfate-depleted sediments in parallel to fermentation and methanogenic metabolisms. The notable abundance of Chloroflexi from the class Dehalococcoidia also suggests alternative sulfur-based metabolic activities by these versatile microorganisms which are hypothesized to be capable of reducing not only sulfate but also organic sulfur compounds (Wasmund et al., 2014; Mehrshad et al., 2018). In fact, Chloroflexi genomes from deep sea sediments have been found to encode for dimethylsulfide, methane sulfonate, and alkane sulfonate metabolisms (Liu et al., 2022). Overall, our findings are consistent with studies on marine sediments demonstrating active sulfate reduction below the zone of sulfate depletion (Holmkvist et al., 2011; Treude et al., 2014; Brunner et al., 2016; Pellerin et al., 2018b) and suggest that deep sulfate reduction also occurs in lake sediments.

https://doi.org/10.5194/egusphere-2023-2102
Preprint. Discussion started: 5 October 2023

An oxidizing front and constant groundwater supply of sulfate at the transition between euxinic and deep glacial deposits appears to sustain continuous microbial sulfur cycling at 600-800 cm depth. Abundant *dsr*B and *sox*B genes there confirm that both microbial sulfate reduction and sulfide oxidation are important. The extremely light $\delta^{34}S$ isotopic composition of CRS and organic S (between -40 and -50 ‰) further support the presence of an active sulfur cycle driven by slow upward diffusion of groundwater sulfate. Sulfate limitation and extremely slow sulfate reduction rates tend to generate extremely light sulfide (Habicht and Canfield, 1997). In addition, multiple reduction and oxidation cycles driven by sulfur-disproportionating bacteria and iron oxides (Canfield and Thamdrup, 1994) can lead to a progressively lighter pool of reduced sulfur. Alternatively, sulfate reduction coupled to methane oxidation (AOM), which generates very large ^{34}S-isotopic fractionations of up to -60 ‰, could be at play (Deusner et al., 2014). In fact, a notable fraction of sulfate-reduction genes recovered at the deep redox transition belong to the methane-oxidizing Methylomirabilota (Fig. 4) which have been known to couple AOM to denitrification (Bhattarai et al., 2019), but whose capacity to perform sulfate-AOM has not been explored. It has further been proposed that deep biosphere sulfate-reducing communities and/or their cellular metabolic activities may be very different than classic sulfate-reducers that have been studied in culture thus far (Wortmann et al., 2001). In this study, we recovered a large number of *dsr*B sequences which could not be annotated at the class or order level (especially in the Deltaproteobacteria) and these novel, unclassified groups could potentially contribute to the large sulfur fractionation values in the Lake Cadagno deep sediments.

4.2 Rapid sulfurization of organic matter and further transformation

Most organic matter degradation in the Lake Cadagno sediment takes place in the upper 40 cm (Berg et al., 2022). There we also observed the greatest changes in sulfur redox chemistry and CRS (which contains pyrite) formation at the expense of both its known mineral precursors

https://doi.org/10.5194/egusphere-2023-2102
Preprint. Discussion started: 5 October 2023

AVS (containing FeS) and elemental sulfur (including polysulfides) (Luther, 1991). The highly significant ($p < 0.001$) enrichment of CRS in lacustrine layers versus mass-movement deposits confirms that most iron sulfides are indeed of authigenic origin resulting from early diagenesis. The rapid sulfurization of organic matter also appears to occur in these < 100 year-old surface sediments which is consistent with other studies of several lakes in Switzerland, in which most organic matter sulfurization was reported to occur within the initial decades after sediment deposition (Urban et al., 1999; Hebting et al., 2006). The recovery of genes involved in sulfur cycling at depth suggests that microorganisms and/or diagenetic processes continue to modify sulfur compounds long after burial thus potentially altering the primary isotopic signal.

Differences in organic matter origin affect organic matter degradation rates and may also affect incorporation of sulfur into organic matter. Support for this comes from the finding that the $\delta^{34}S$ of organic S in lacustrine layers is significantly lower ($p < 0.01$) than that in mass-movement deposits. Small differences in C:N ratios in lacustrine sediment (10.55 ± 1.39) compared to in mass movement deposits (13.75 ± 1.68) suggest that there are clear organic matter compositional differences ($p < 0.01$ significance, Student's t-test) between these two different types of sediment deposits. Alternatively, the more negative $\delta^{34}S$ signatures of deep lacustrine sediment layers compared to event deposits could also be due to post-depositional differences in sulfate reduction rates which have been shown to be sensitive to organic matter quality (Glombitza et al., 2013).

4.3 Competition between organic matter sulfurization versus pyritization and large S isotope fractionations

While it is assumed that Fe-rich sediments favor the precipitation of iron sulfides over the formation of organic S, the competition between these reactions has never been studied in detail. In the Lake Cadagno sediment, there are consistent and significant ($p < 0.01$) differences

https://doi.org/10.5194/egusphere-2023-2102
Preprint. Discussion started: 5 October 2023

between the $\delta^{34}S$ signatures of CRS and organic S suggesting the differential timing of formation of these two phases, for example in the water column versus in sediments (Raven et al., 2023). It is also possible that the slower rate of organic matter sulfurization generates greater isotopic fractionation than the rapid precipitation of iron sulfide (Price and Shieh, 1979; Butler et al., 2004). The HAS fraction in Lake Cadagno sediments may thus be enriched in more negative S left behind after pyrite formation. This organic S (HAS) forms despite the excess of Fe^{2+} favoring the precipitation of inorganic sulfides minerals (CRS, AVS) throughout most of the euxinic mid-column sediments. Indeed, simultaneous organic sulfur and iron sulfide formation has been observed experimentally (Raven et al., 2021). Pyritization of metastable iron sulfide minerals follows a dissolution-precipitation pathway and it is therefore possible that these secondary reactions alter the S-isotopic composition of initial precipitates, as evidenced by differences between AVS and CRS pools in the surface sediments (Fig. 2D). These secondary reactions are restricted to mineral surfaces (Liu et al., 2020) allowing δ34S-CRS values to be preserved in deeper sediments, down to the zone impacted by groundwater sulfate seepage.

A comparison of Lake Cadagno organic sulfur and pyrite $\delta^{34}S$ with profiles from other sediments (e.g. (Goldhaber and Kaplan, 1980; Werne et al., 2003; Raven et al., 2016, 2023) reveals contrasting trends. In Cretaceous ocean sediments, for example, it was found that the degree of organic matter sulfurization was correlated with anoxic water column conditions (Raven et al., 2019). While organic sulfur $\delta^{34}S$ values were relatively constant with depth, pyrite $\delta^{34}S$ was generally lighter and varied as a function of local Fe supply. In more recent marine sediments, local microbial sulfate reduction and isotopic exchange of organic sulfur with porewater sulfide (Raven et al., 2016) have been postulated to control sulfur isotope pools. In contrast, the deeply buried organic sulfur $\delta^{34}S$ in Lake Cadagno is relatively lighter and more variable than pyrite. This suggests that controls on sulfur partitioning into organic sulfur and

https://doi.org/10.5194/egusphere-2023-2102
Preprint. Discussion started: 5 October 2023

pyrite fractions are not yet completely understood or that sulfur cycling mechanisms are very specific to the local biogeochemical environment. Further studies to elucidate the reaction kinetics governing iron- and organic-bound sulfur may help resolve observed discrepancies between dissolved sulfide, organic sulfur, and pyrite $\delta^{34}S$ signatures and contribute to a more accurate interpretation of the geological record.

5. CONCLUSION

This study reveals that microbial sulfur cycling in sulfate-depleted sediments may be a common phenomenon not restricted to marine sediments. This deep sulfur cycling appears to be driven by a diverse, and uncultivated biosphere, as most *dsr*B lineages recovered here belong to novel taxa whose role in sulfur and carbon cycling has yet to be revealed. These microorganisms, such as Chloroflexi, are not classical sulfate-reducing bacteria that have been characterized thus far in the laboratory. Due to the dominance of these uncultivated lineages in the Lake Cadagno sediments and the extreme S isotope signatures observed, understanding the ecophysiology and metabolism of these novel microorganisms will be important to interpreting sulfur isotopes in the geological record.

In addition to microbial isotope fractionation effects during sulfate reduction, our findings show that different reduced sulfur pools preserve distinct S isotopic signatures, which is possibly related to different kinetics of formation or subsequent chemical or microbial transformations. We have specifically documented a diagenetic effect on pyrite formation with large S isotope differences generated by local geochemical conditions. Indeed, it has recently been pointed out that there are very local influences on pyrite isotope composition which have important implications for interpretations of the global geological record (Pasquier et al., 2021). Organic sulfur versus pyrite formation appears to vary across environments and be related to organic matter content, aqueous sulfide and reactive iron availability.

https://doi.org/10.5194/egusphere-2023-2102
Preprint. Discussion started: 5 October 2023

6. ACKNOWLEDGEMENTS

We thank the entire 2019 Cadagno sampling crew for assistance in the field, and especially the Alpine Biology Center Foundation (Switzerland) for use of its research facilities. We also acknowledge Iso Christl, Rachele Ossola, and Jorge Spangenberg for their support with chemical analyses. This study was supported by the Swiss National Science Foundation (SNF) grant No. 182096 (M.A.L.).

7. CONFLICT OF INTEREST

The authors declare no conflict of interest.

8. DATA AVAILABILITY

dsrB gene sequences have been deposited in the NCBI database under Bioproject number PRJNA991470. All other raw data has been deposited in SWISSUbase under study number 20541.

9. AUTHOR CONTRIBUTIONS

JSB performed sediment sampling and chemical analyses, synthesized the data and wrote the manuscript. PCR and LD performed microbial community analyses and interpretations under supervision of CM. SB provided S-isotope data from 1991 and 2019. HV and MM performed sediment sampling and sedimentological characterizations and dating. MAL supervised this project.

REFERENCES

Anantharaman K., Hausmann B., Jungbluth S. P., Kantor R. S., Lavy A., Warren L. A., Rappé M. S., Pester M., Loy A., Thomas B. C. and Banfield J. F. (2018) Expanded diversity of microbial groups that shape the dissimilatory sulfur cycle. *ISME J* **12**, 1715–1728.

Berg J. S., Lepine M., Laymand E., Han X., Vogel H., Morlock M. A., Gajendra N., Gilli A., Bernasconi S. M., Schubert C. J., Su G. and Lever M. A. (2022) Ancient and Modern Geochemical Signatures in the 13,500-Year Sedimentary Record of Lake Cadagno. *Frontiers in Earth Science* **9**.

https://doi.org/10.5194/egusphere-2023-2102
Preprint. Discussion started: 5 October 2023

Bernasconi S. M., Meier I., Wohlwend S., Brack P., Hochuli P. A., Bläsi H., Wortmann U. G. and Ramseyer K. (2017) An evaporite-based high-resolution sulfur isotope record of Late Permian and Triassic seawater sulfate. *Geochimica et Cosmochimica Acta* **204**, 331–349.

Bhattarai S., Cassarini C. and Lens P. N. L. (2019) Physiology and Distribution of Archaeal Methanotrophs That Couple Anaerobic Oxidation of Methane with Sulfate Reduction. *Microbiology and Molecular Biology Reviews* **83**, 10.1128/mmbr.00074-18.

Bowles M. W., Mogollón J. M., Kasten S., Zabel M. and Hinrichs K.-U. (2014) Global rates of marine sulfate reduction and implications for sub–sea-floor metabolic activities. *Science* **344**, 889–891.

Bradley A. S., Leavitt W. D., Schmidt M., Knoll A. H., Girguis P. R. and Johnston D. T. (2016) Patterns of sulfur isotope fractionation during microbial sulfate reduction. *Geobiology* **14**, 91–101.

Brunner B., Arnold G. L., Røy H., Müller I. A. and Jørgensen B. B. (2016) Off Limits: Sulfate below the Sulfate-Methane Transition. *Front. Earth Sci.* **4**.

Brunner B. and Bernasconi S. M. (2005) A revised isotope fractionation model for dissimilatory sulfate reduction in sulfate reducing bacteria. *Geochimica et Cosmochimica Acta* **69**, 4759–4771.

Butler I. B., Böttcher M. E., Rickard D. and Oldroyd A. (2004) Sulfur isotope partitioning during experimental formation of pyrite via the polysulfide and hydrogen sulfide pathways: implications for the interpretation of sedimentary and hydrothermal pyrite isotope records. *Earth and Planetary Science Letters* **228**, 495–509.

Canfield D. E. (2004) The evolution of the Earth surface sulfur reservoir. *Am J Sci* **304**, 839–861.

Canfield D. E., Farquhar J. and Zerkle A. L. (2010) High isotope fractionations during sulfate reduction in a low-sulfate euxinic ocean analog. *Geology* **38**, 415–418.

Canfield D. E. and Thamdrup B. (1994) The production of 34S-depleted sulfide during bacterial disproportionation of elemental sulfur. *Science* **266**, 1973–1975.

Cypionka H., Smock A. M. and Böttcher M. E. (1998) A combined pathway of sulfur compound disproportionation in Desulfovibrio desulfuricans. *FEMS Microbiology Letters* **166**, 181–186.

Damsté J. S. and De Leeuw J. W. (1990) Analysis, structure and geochemical significance of organically-bound sulphur in the geosphere: State of the art and future research. *Organic Geochemistry* **16**, 1077–1101.

David M. B. and Mitchell M. J. (1985) Sulfur constituents and cycling in waters, seston, and sediments of an oligotrophic lake. *Limnology and Oceanography* **30**, 1196–1207.

Deng L., Meile C., Fiskal A., Bölsterli D., Han X., Gajendra N., Dubois N., Bernasconi S. M. and Lever M. A. (2022) Deposit-feeding worms control subsurface ecosystem functioning in intertidal sediment with strong physical forcing. *PNAS Nexus* **1**, pgac146.

Detmers J., Brüchert V., Habicht K. S. and Kuever J. (2001) Diversity of Sulfur Isotope Fractionations by Sulfate-Reducing Prokaryotes. *Appl. Environ. Microbiol.* **67**, 888–894.

https://doi.org/10.5194/egusphere-2023-2102
Preprint. Discussion started: 5 October 2023

Deusner C., Holler T., Arnold G. L., Bernasconi S. M., Formolo M. J. and Brunner B. (2014) Sulfur and oxygen isotope fractionation during sulfate reduction coupled to anaerobic oxidation of methane is dependent on methane concentration. *Earth and Planetary Science Letters* **399**, 61–73.

Ferdelman T. G., Church T. M. and Luther G. W. (1991) Sulfur enrichment of humic substances in a Delaware salt marsh sediment core. *Geochimica et Cosmochimica Acta* **55**, 979–988.

Fike D. A., Bradley A. S. and Rose C. V. (2015) Rethinking the Ancient Sulfur Cycle. *Annual Review of Earth and Planetary Sciences* **43**, 593–622.

Fossing H. and Jørgensen B. B. (1989) Measurement of bacterial sulfate reduction in sediments: Evaluation of a single-step chromium reduction method. *Biogeochemistry* **8**, 205–222.

Glombitza C., Stockhecke M., Schubert C. J., Vetter A. and Kallmeyer J. (2013) Sulfate reduction controlled by organic matter availability in deep sediment cores from the saline, alkaline Lake Van (Eastern Anatolia, Turkey). *Front Microbiol* **4**, 209.

Goldhaber M. B. and Kaplan I. R. (1980) Mechanisms of sulfur incorporation and isotope fractionation during early diagenesis in sediments of the gulf of California. *Marine Chemistry* **9**, 95–143.

Habicht K. S. and Canfield D. E. (2001) Isotope fractionation by sulfate-reducing natural populations and the isotopic composition of sulfide in marine sediments. *Geology* **29**, 555–558.

Habicht K. S. and Canfield D. E. (1997) Sulfur isotope fractionation during bacterial sulfate reduction in organic-rich sediments. *Geochimica et Cosmochimica Acta* **61**, 5351–5361.

Hebting Y., Schaeffer P., Behrens A., Adam P., Schmitt G., Schneckenburger P., Bernasconi S. M. and Albrecht P. (2006) Biomarker Evidence for a Major Preservation Pathway of Sedimentary Organic Carbon. *Science* **312**, 1627–1631.

Holmkvist L., Kamyshny A., Vogt C., Vamvakopoulos K., Ferdelman T. G. and Jørgensen B. B. (2011) Sulfate reduction below the sulfate–methane transition in Black Sea sediments. *Deep Sea Research Part I: Oceanographic Research Papers* **58**, 493–504.

Jochum L. M., Chen X., Lever M. A., Loy A., Jørgensen B. B., Schramm A. and Kjeldsen K. U. (2017) Depth Distribution and Assembly of Sulfate-Reducing Microbial Communities in Marine Sediments of Aarhus Bay. *Appl. Environ. Microbiol.* **83**.

Johnston D. T. (2011) Multiple sulfur isotopes and the evolution of Earth's surface sulfur cycle. *Earth-Science Reviews* **106**, 161–183.

Johnston D. T., Farquhar J. and Canfield D. E. (2007) Sulfur isotope insights into microbial sulfate reduction: When microbes meet models. *Geochimica et Cosmochimica Acta* **71**, 3929–3947.

Jørgensen B. B. (1982) Mineralization of organic matter in the sea bed—the role of sulphate reduction. *Nature* **296**, 643–645.

Kallmeyer J., Ferdelman T. G., Weber A., Fossing H. and Jørgensen B. B. (2004) A cold chromium distillation procedure for radiolabeled sulfide applied to sulfate reduction measurements. *Limnology and Oceanography: Methods* **2**, 171–180.

https://doi.org/10.5194/egusphere-2023-2102
Preprint. Discussion started: 5 October 2023

Klein M., Friedrich M., Roger A. J., Hugenholtz P., Fishbain S., Abicht H., Blackall L. L., Stahl D. A. and Wagner M. (2001) Multiple Lateral Transfers of Dissimilatory Sulfite Reductase Genes between Major Lineages of Sulfate-Reducing Prokaryotes. *Journal of Bacteriology* **183**, 6028–6035.

Lever M. A., Rouxel O., Alt J. C., Shimizu N., Ono S., Coggon R. M., Shanks W. C., Lapham L., Elvert M., Prieto-Mollar X., Hinrichs K.-U., Inagaki F. and Teske A. (2013) Evidence for Microbial Carbon and Sulfur Cycling in Deeply Buried Ridge Flank Basalt. *Science* **339**, 1305–1308.

Lever M. A., Torti A., Eickenbusch P., Michaud A. B., Šantl-Temkiv T. and Jørgensen B. B. (2015) A modular method for the extraction of DNA and RNA, and the separation of DNA pools from diverse environmental sample types. *Front. Microbiol.* **6**.

Liu J., Pellerin A., Antler G., Kasten S., Findlay A. J., Dohrmann I., Røy H., Turchyn A. V. and Jørgensen B. B. (2020) Early diagenesis of iron and sulfur in Bornholm Basin sediments: The role of near-surface pyrite formation. *Geochimica et Cosmochimica Acta* **284**, 43–60.

Liu R., Wei X., Song W., Wang L., Cao J., Wu J., Thomas T., Jin T., Wang Z., Wei W., Wei Y., Zhai H., Yao C., Shen Z., Du J. and Fang J. (2022) Novel Chloroflexi genomes from the deepest ocean reveal metabolic strategies for the adaptation to deep-sea habitats. *Microbiome* **10**, 75.

Luther G. W. (1991) Pyrite synthesis via polysulfide compounds. *Geochimica et Cosmochimica Acta* **55**, 2839–2849.

Mehrshad M., Rodriguez-Valera F., Amoozegar M. A., López-García P. and Ghai R. (2018) The enigmatic SAR202 cluster up close: shedding light on a globally distributed dark ocean lineage involved in sulfur cycling. *ISME J* **12**, 655–668.

Meyer B., Imhoff J. F. and Kuever J. (2007) Molecular analysis of the distribution and phylogeny of the soxB gene among sulfur-oxidizing bacteria – evolution of the Sox sulfur oxidation enzyme system. *Environmental Microbiology* **9**, 2957–2977.

Mitchell M. J., Landers D. H. and Brodowski D. F. (1981) Sulfur constituents of sediments and their relationship to lake acidification. *Water Air Soil Pollut* **16**, 351–359.

Müller A. L., Kjeldsen K. U., Rattei T., Pester M. and Loy A. (2015) Phylogenetic and environmental diversity of DsrAB-type dissimilatory (bi)sulfite reductases. *The ISME Journal* **9**, 1152–1165.

Nriagu J. O. and Soon Y. K. (1985) Distribution and isotopic composition of sulfur in lake sediments of northern Ontario. *Geochimica et Cosmochimica Acta* **49**, 823–834.

Orr W. L. and Damsté J. S. (1990) Geochemistry of Sulfur in Petroleum Systems. In *Geochemistry of Sulfur in Fossil Fuels* ACS Symposium Series. American Chemical Society. pp. 2–29.

Paiste K., Lepland A., Zerkle A. L., Kirsimäe K., Kreitsmann T., Mänd K., Romashkin A. E., Rychanchik D. V. and Prave A. R. (2020) Identifying global vs. basinal controls on Paleoproterozoic organic carbon and sulfur isotope records. *Earth-Science Reviews* **207**, 103230.

Pasquier V., Bryant R. N., Fike D. A. and Halevy I. (2021) Strong local, not global, controls on marine pyrite sulfur isotopes. *Science Advances* **7**, eabb7403.

https://doi.org/10.5194/egusphere-2023-2102
Preprint. Discussion started: 5 October 2023

Pellerin A., Antler G., Røy H., Findlay A., Beulig F., Scholze C., Turchyn A. V. and Jørgensen B. B. (2018a) The sulfur cycle below the sulfate-methane transition of marine sediments. *Geochimica et Cosmochimica Acta* **239**, 74–89.

Pellerin A., Antler G., Røy H., Findlay A., Beulig F., Scholze C., Turchyn A. V. and Jørgensen B. B. (2018b) The sulfur cycle below the sulfate-methane transition of marine sediments. *Geochimica et Cosmochimica Acta* **239**, 74–89.

Pester M., Knorr K.-H., Friedrich M. W., Wagner M. and Loy A. (2012) Sulfate-reducing microorganisms in wetlands – fameless actors in carbon cycling and climate change. *Front. Microbiol.* **3**.

Price F. T. and Shieh Y. N. (1979) Fractionation of sulfur isotopes during laboratory synthesis of pyrite at low temperatures. *Chemical Geology* **27**, 245–253.

Raven M. R., Crockford P. W., Hodgskiss M. S. W., Lyons T. W., Tino C. J. and Webb S. M. (2023) Organic matter sulfurization and organic carbon burial in the Mesoproterozoic. *Geochimica et Cosmochimica Acta* **347**, 102–115.

Raven M. R., Fike D. A., Bradley A. S., Gomes M. L., Owens J. D. and Webb S. A. (2019) Paired organic matter and pyrite δ34S records reveal mechanisms of carbon, sulfur, and iron cycle disruption during Ocean Anoxic Event 2. *Earth and Planetary Science Letters* **512**, 27–38.

Raven M. R., Keil R. G. and Webb S. M. (2021) Rapid, Concurrent Formation of Organic Sulfur and Iron Sulfides During Experimental Sulfurization of Sinking Marine Particles. *Global Biogeochemical Cycles* **35**, e2021GB007062.

Raven M. R., Sessions A. L., Fischer W. W. and Adkins J. F. (2016) Sedimentary pyrite δ34S differs from porewater sulfide in Santa Barbara Basin: Proposed role of organic sulfur. *Geochimica et Cosmochimica Acta* **186**, 120–134.

Rudd J. W. M., Kelly C. A. and Furutani A. (1986) The role of sulfate reduction in long term accumulation of organic and inorganic sulfur in lake sediments1. *Limnology and Oceanography* **31**, 1281–1291.

Schubert C. J., Vazquez F., Lösekann-Behrens T., Knittel K., Tonolla M. and Boetius A. (2011) Evidence for anaerobic oxidation of methane in sediments of a freshwater system (Lago di Cadagno). *FEMS Microbiol Ecol* **76**, 26–38.

Sim M. S., Bosak T. and Ono S. (2011) Large Sulfur Isotope Fractionation Does Not Require Disproportionation. *Science* **333**, 74–77.

Slobodkin A. I. and Slobodkina G. B. (2019) Diversity of Sulfur-Disproportionating Microorganisms. *Microbiology* **88**, 509–522.

Steingruber S. M., Bernasconi S. M. and Valenti G. (2020) Climate Change-Induced Changes in the Chemistry of a High-Altitude Mountain Lake in the Central Alps. *Aquat Geochem*.

Treude T., Krause S., Maltby J., Dale A. W., Coffin R. and Hamdan L. J. (2014) Sulfate reduction and methane oxidation activity below the sulfate-methane transition zone in Alaskan Beaufort Sea continental margin sediments: Implications for deep sulfur cycling. *Geochimica et Cosmochimica Acta* **144**, 217–237.

https://doi.org/10.5194/egusphere-2023-2102
Preprint. Discussion started: 5 October 2023

629 Urban N. R., Ernst K. and Bernasconi S. (1999) Addition of sulfur to organic matter during early
630 diagenesis of lake sediments. *Geochimica et Cosmochimica Acta* **63**, 837–853.

631 Vuillemin A., Kerrigan Z., D'Hondt S. and Orsi W. D. (2020) Exploring the abundance, metabolic
632 potential and gene expression of subseafloor Chloroflexi in million-year-old oxic and anoxic
633 abyssal clay. *FEMS Microbiology Ecology* **96**, fiaa223.

634 Wasmund K., Schreiber L., Lloyd K. G., Petersen D. G., Schramm A., Stepanauskas R., Jørgensen B. B.
635 and Adrian L. (2014) Genome sequencing of a single cell of the widely distributed marine
636 subsurface Dehalococcoidia, phylum Chloroflexi. *ISME J* **8**, 383–397.

637 Werne J. P., Lyons T. W., Hollander D. J., Formolo M. J. and Sinninghe Damsté J. S. (2003) Reduced
638 sulfur in euxinic sediments of the Cariaco Basin: sulfur isotope constraints on organic sulfur
639 formation. *Chemical Geology* **195**, 159–179.

640 Wirth S. B., Gilli A., Niemann H., Dahl T. W., Ravasi D., Sax N., Hamann Y., Peduzzi R., Peduzzi S.,
641 Tonolla M., Lehmann M. F. and Anselmetti F. S. (2013) Combining sedimentological, trace
642 metal (Mn, Mo) and molecular evidence for reconstructing past water-column redox
643 conditions: The example of meromictic Lake Cadagno (Swiss Alps). *Geochimica et*
644 *Cosmochimica Acta* **120**, 220–238.

645 Wortmann U. G., Bernasconi S. M. and Böttcher M. E. (2001) Hypersulfidic deep biosphere indicates
646 extreme sulfur isotope fractionation during single-step microbial sulfate reduction. *Geology*
647 **29**, 647–650.

648

649